ISSN: 2710-2165

Predicting the Performance of Solar Water Heater using Thermal Performance Enhancers

Hussein A. Mahmood[*], Ali D. Salman[**], Mohammed F. Mohammed[***]

[*] Mechanical Engineering, University of Technology, Iraq
Email: me.20.10@grad.uotechnology.edu.iq
https://orcid.org/0009-0000-4637-5164

[**] Mechanical Engineering, University of Technology, Iraq
Email: ali.d.salman@uotechnology.edu.iq
https://orcid.org/0000-0003-2742-1852

[***] Mechanical Engineering, University of Technology, Iraq
Email: 20011@uotechnology.edu.iq
https://orcid.org/0000-0003-4582-468X

Abstract

In this study, a practical study was conducted to compare the efficient behavior of close loop solar water heater with thermosiphon- riser tubes with dimensions (80 cm width, 120 cm height) with two acrylic covering. both with and without thermal performance enhancer, and to find the optimum mode of convection in the collector. the thermal performance enhancers have been used, helical spring with a core bar, and they were inserted a solar absorber tube The ethanol as a working fluid is used by applying a practical test set to it. The current tests were conducted on September 6, 8 and October 4, 5 , 2022, in Baghdad, Iraq, under identical ambient and load circumstances. All examination were from 08:00 am to 16:00 pm, at tilted angle (45 °) South in sunny days. The experimental tests were carried out at flow rates (1 and 1.5 L/min) and filling ratio (50%). At a flow rate of 1.5 L/min and a filling ratio of 50%, using an inserted helical spring with a core bar yielded the highest daily efficiency of 70%. In the interest of the system.

Keywords- ethanol,filling ratio, thermosiphon, thermal performance enhancers ,water heater.

I. INTRODUCTION

Thermosiphon solar water heating systems don't need to utilize any pumping energy, they are the most cost-effective heating equipment. Samanci and Berber [1] performed an experimental study comparing the efficiency of single-phase (water and two-phase) and R-134a (heating and cooling) systems with comparable specifications. It was shown that two-Phase systems had a 42.8% improvement in performance over single-Phase ones. The effectiveness of a water-filled, closed thermosiphon was found to be unaffected by the device's tilt or filled ratio. An evaporator with a water chiller and a 65 C jacket was investigated by Ong et al. The dynamic modeling of a thermosyphon solar water heater was explored [3] with consideration given to the environment of a city in northern Iran. Both sunny and cloudy days were accounted for in the simulated weather. We measured the absorber and glass cover center and input and outlet temperatures, as well as gathered efficiency diagrams and usable energy. Air temperature, sun radiation, wind and rain impacts, and so forth all affect thermal performance, [4]. Thermosiphon solar water heaters may either be single- or two-phase. These heaters' heating efficiency is dependent on the working fluid's phase. For domestic and commercial usage, [5] researchers have designed a solar water heater that also functions as a solar heat collector. Benefits include cheap cost per kilowatt hour, great efficiency, and a high level of stability between the solar heating side and the water-cooling side. System characteristics of a two-phase closed loop thermosyphon solar water heater have been studied numerically [6] to see how riser diameter and riser inclination angle affect the system. The diameter of the riser tubes ranged from 1.25 to 2.5 cm, and their slant ranged from 2 to 75 degrees.For a split-type solar water heater [7], an insert-type two-phase closed loop thermosyphon (or gravity return loop heat pipe) was developed to cut down on installation and maintenance hassles.. The proposed insert-type loop thermosyphon outperforms conventional thermosyphons in two key respects: heat transit limit and beginning speed.. The filling ratio greatly affected its heat resistance, flow patterns, and behavior at starting. In order to learn how filling ratio impacts thermosiphons' transient performance, Shabgard et al. [8] created a mathematical model. Working parameters, maximum heat transfer rate, and total thermal resistance of the TPCT have been determined using a built and functional experimental facility [9].. Research was conducted using heat transfer coefficients of 30-700 W and filling ratios of 16-35- and 135%. For the first time, research [10] has anticipated the geyser-boiling regime and two-phase pattern that happens with water at low power throughput. The multiphase flow characteristics of the condenser e heat exchanger might be modeled and shown with the help of the CFD simulation. A model consisting of the Volume of Fluid (VOF) model, the phase change model, and the continuum surface force

ISSN: 2710-2165

model was built to replicate the features of heat transfer [11]. Free cooling based on loop thermosyphon may help data centers save electricity. In order to promote its widespread use in the future, it is crucial to examine how well employing environmentally friendly working fluids functions. The results of this investigation show that relative errors may be minimized by including a temporal relaxation parameter for transient mass transfer in the model. The superheated zone decreases and disappears, as seen by thermal imaging, as the filling ratio increases. By combining heat pipes with conventional flat plate collectors, an alternative to conventional HVAC has been introduced. The worst-case performance was analyzed using dynamic simulations. In a recent publication [14], researchers analyzed the unique, compact evacuated heat pipe solar water heater that is combined with a latent heat storage tank. The suggested approach improved the average efficiency of three distinct PCMs from about 10% to 58.5% over the baseline. We developed [15], constructed (and tested) a new shell and tube latent heat storage device to use in tandem with the flat plate solar water heater. The experiment results showed that a combination of PCM and water storage tanks had the highest daily efficiency of 65 percent. Smaller thermosyphons are increasingly sought after as electronic component coolers [16]. High-speed videography allowed us to see the flow patterns in real time at different heat input powers. Higher temperatures were observed to result in more severe boiling events because less liquid returned to the evaporator. The results of the performance analysis [17] validated the use of a specially designed photovoltaic (PV) panel and a certain kind of solar water heater in conjunction with a wickless heat pipe. Five water pipe loops were shown to be potentially ideal for heating a tank in a simulation of a passive photovoltaics (PVT) solar system. Tank water temperature peaked in the evening at about 72 degrees Celsius and was maintained at around 70 degrees Celsius throughout operation. Different heat loads, mass flow rates, and cooling water input temperatures have all been studied in relation to geyser boiling. The effect of fill ratios and inclination angles (90, 60, 30, and 10 degrees) has also been investigated [18]. Fill ratios of 100 percent result in shorter times at 90, 30, and 10 degree angles than fill ratios of 25 and 65 percent. A mathematical model of the natural circulation phenomena [19] has been used to effectively describe the solar thermosyphon, also known as a solar wind turbine. In order to test the solar thermoplane, the confirmed model was run with different tilt angles, geometries, and operating circumstances. It can estimate how much solar radiation and how much of an angle of tilt are necessary to increase flow. Researchers looked several ways to improve the thermal performance of flat-plate collectors [20]. In the experiment, a standard circular tube and a twisted tube with a range of cross sections were used to create a heat exchanger. When using both pure water and MWCNT/water as the nanofluid, twisted tubes achieved 12.8 and 12.5% more performance than their circular counterparts. The MWCNT-wired tubes outperformed the conventional water-filled tubes in every metric. By reducing the evaporator temperature, nanofluids in thermosyphons are shown to improve thermal performance numerically [21]. Reason being, they cut down on entropy production by 41% for Cu and 32% for Fe2O3, respectively. Maximum friction entropy production rises by around 36.37 percent for Cu, 15.15 percent for Fe2O3, and 9.09 percent for Al2O3 at = 9 weight percent. In addition, increasing the concentration of nanoparticles has a negative impact on entropy production. To improve the thermosyphon system's thermal performance, researchers have used both computational and experimental methods [22]. Experimental data and the classic model for fluid dynamics accord well, as proved by numerical simulations. According to studies conducted at Scotland's University of Aberdeen, both of these models have temperature responses that are bigger than those of a conventional model. A 50% optimum filling ratio (OFR) was found to minimize thermal resistance by 22.2% and evaporator wall temperature by 9.31% [23]. Low pressure and high heat transfer rates at OFR reduced entropy production by 12.6 and 16.6 percent, respectively. Surface area and evaporation rate are both increased by the internal MPMC fins, which also improve heat transport and hence minimize entropy formation [24]. The effectiveness of the simple closed thermosiphon (SCT) in transmitting heat (1 kW) at varying adiabatic heights was evaluated (0.25, 1, and 1.5 m). Compared to the heat obtained by SCT, the heat generated by the Thermal Transfer Device (THTD) is 1.5 times stronger. In order to experimentally examine THTD's performance, we varied coolant flow rates, loads, and transport distances. The resulting energy efficiency was anywhere between 80% and 90%. Effective thermal conductivity in Type III evaporators is the highest (6.123e+05 W/m°C) and thermal resistance is reduced by the most (37.32%) [from its initial value]. The heat transmission coefficient of 2456 W/m2.°C is greater than that of the preceding two types.. When compared to other fluids, the efficiency and low values (up to 72% reduction in total thermal resistance) of an acetone-charged loop thermosyphon were striking [26]. The plate-type forced air-cooled condenser had the maximum heating and cooling efficiency.. Because of this, the loop thermosyphon with a plate-type forced air-cooled condenser was seen as an adequate solution to the problem of overheating in electronic components, computer clusters, and data centers when using a water-cooled condenser. Mohamed et al. [27] report doing an outdoor experiment at the Menoufia University Faculty of Engineering in Shiben El-kom, Egypt (about 30.58 degrees North and 31.01 degrees East). Heat pipe systems using acetone and ethanol as the working fluids were employed to transfer energy from the solar collectors to the storage tank. Theoretical calculations put the traditional system's efficiency between 50 and 53 percent, while its actual performance fell in the 47 to 53 percent range [28]. Two types of working fluids (acetone and ethanol) and a wide range of heat pipe counts were used. Solar water heaters transfer heat from the absorber plate to the storage tank through heat pipes.

In order to store steam, this concept plans to use ethanol as the working fluid in a thermosiphon arrangement. The purpose of this experiment was to compare the efficiency of solar water heaters with and without thermal performance enhancers employing thermosiphon-riser collectors at two different water flow rates (1 and 1.5 L/min) (50 percent ,).

ISSN: 2710-2165

II. MATHEMATICAL MODELING

Figure (1) depicts the experimental test rig, and Table (1) provides a detailed schematic layout of the thermosiphon riser solar collector. The solar collector has a matte-painted solar absorber (80 by 120 cm) and a double acrylic layers thickness (4 mm) that faces south and is slanted at an angle of 45 degrees. An absorber of solar radiation, made of copper sheet (0.5 mm thick). Also included are eight parallel copper pipes (using eight parallel copper pipes According to literature review 4) that are each (120 cm) long, (10.5 mm) in diameter, and (11.5 mm) in diameter. The distance between the cores of two adjacent tubes (10 cm). Two more headers, one at each end, connect these pipes to the top and lower levels. Copper pipes with an outer diameter of (41 mm) and a total length of (100 mm) make up the top header (80 cm). The bottom header is 80 centimeters in length and (6.25 mm) in diameter. The riser pipes are welded to the absorbent plate with lead. Reducing the heat loss from the collector's sides and bottom A thermal insulator consisting of (50 mm) of glass wool insulation. Metal bars (1.5 mm thick) form the collection's (92 by 137 cm) frame. The collector sides are thermally insulated with (25 mm)of glass wool to reduce heat losses.A (1mm) insulated capillary tube panel links the top header to the pressure gauge and chargeable valve, allowing the non-condensable gas to be vented and the ethanol to be charged as the working fluid.. The dimensions of the sub cool heat exchanger tubes utilized were (12.7 mm) length (25 mm) outer diameter. The steam tank is linked to the collector through the pump and is responsible for condensing the bulk of the ethanol vapor (using ethanol alcohol as a working fluid According to literature review 28) before any of it reaches the water tank. The condensed liquid then returns to the collection by gravity. (11)Thermocouples and an Arduino Mega 256 The water entrance and exit, the evaporator and condenser, the ends and the center of the absorbent plate, and the clear cover are all measured using a K-type thermometer. The solar meter measures the incident solar power radiation on the collector from 0 to 2000 W/m2. A modest circulation pump (DC 24v) moves water through the system at a rate of (0.1 to 0.3 L/ min) and may lift water to a height of (3 m). All of the measuring tools used in this research were checked and adjusted for accuracy before we headed out into the field.

The equation was used to compute the water flow rate [29].

$$\dot{m}_w = \rho_w \cdot \dot{V}_w \quad (1)$$

The calculation of the useful energy across a collector during a half-hour is as follows, Duffie and Beackman[29].

$$Q_u = \dot{m}_w \cdot C_w \cdot (T_{out} - T_{in}) \quad (2)$$

Trapezoidal rule has been used to calculate the daily useful energy (Q_{ud}) and the daily solar radiation (G_{Td}),

$$Q_{ud} = b\left[\frac{Q_{u1}}{2} + Q_{u2} + Q_{u3} + \cdots + \frac{Q_{un}}{2}\right] \quad (3)$$

b = increments of time = 1,800 seconds

$$G_{Td} = A_c \cdot b\left[\frac{G_{T1}}{2} + G_{T2} + G_{T3} + \cdots + \frac{G_{Tn}}{2}\right] \quad (4)$$

The daily efficiency can be calculated [29].

$$\eta_d = \frac{Q_{ud}}{G_{Td}} \quad (5)$$

To calculate the instantaneous efficiency [29].

ISSN: 2710-2165

$$\eta_i = \frac{Q_u}{A_c . G_T} \quad (6)$$

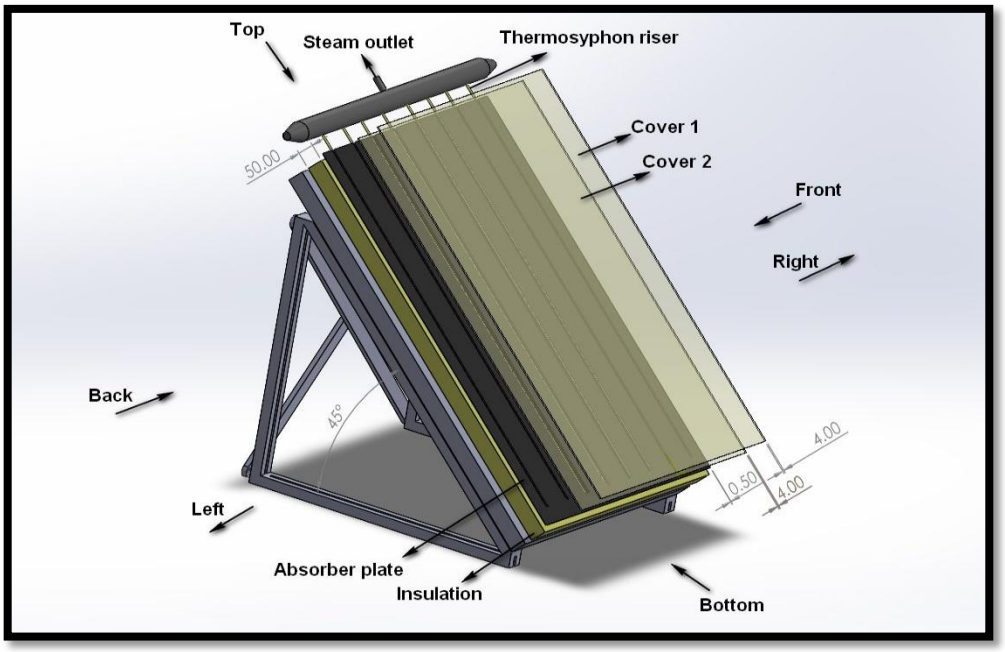

(a) The collector of solar water heater with a thermosiphon

No	Parameters	Specification
1	Tubs	Do = 10.5 mm
	Upper header	Do = 41 mm
	Lower header	Do = 6.35 mm
2	Charge	Do = 6.35 mm
3	valve	Do = 6.35 mm boll valve
4	Flexible tube	Di =8mm
5	Gauge pressure	2 bars
6	Discharge pipe	Do = 6.35 mm
7	Subcool Heat Exchange Pipe Installed	Do = 7.9 mm
8	Heat exchange	Do = 6.35 mm, L = 2 m
9	Steam tank	Di = 20 cm, L = 30 cm
10	Sub cool Heat exchange	Do = 12.7 mm, L = 25 mm
11	Water pump	500 L /h
12	Flow meter Water	200 L/h
13	Storage tank Hot Water	40 L
14	Feed tank of water	25 L
15	Cylinder with a graduated transparency	Di = 5 cm, h = 25 cm
16	Transparent Graduated tank	600 cc
17	Transparent Graduated tube for level of working fluid	Do = 12.7 mm
18	thermocouples	°C

ISSN: 2710-2165

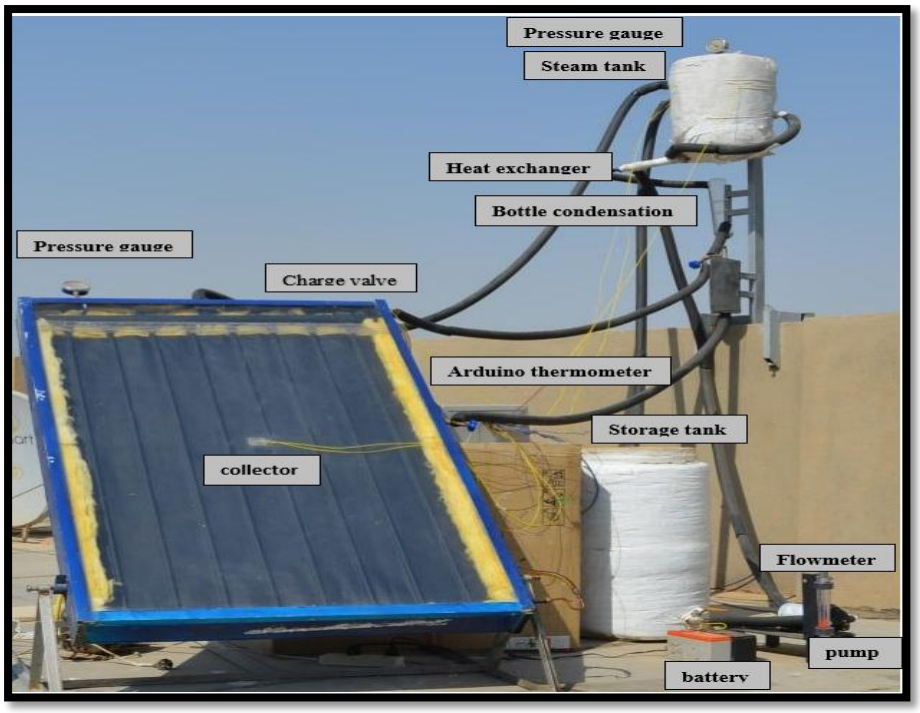

(b) photograph of the solar water heater collector with a thermosiphon

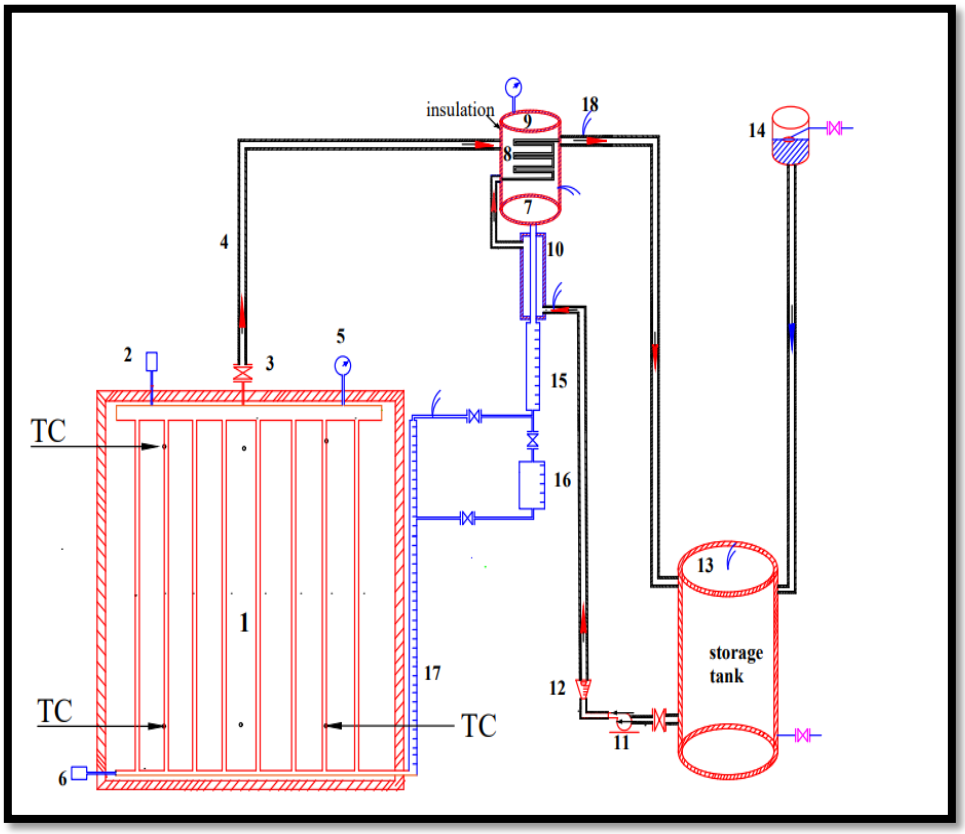

(c) Schematic diagram of the solar water heater with a thermosiphon

Figure (1) Solar water heater with ethanol thermosiphon-riser collector

ISSN: 2710-2165

III. RESULTS AND DISCUSSION

Effect of filling ratio on useful energy

Figures (2 & 3) represents solar energy conversion efficiency and filling time (50 percent) with and without a helical spring put into the core. variations in closed-loop flow rates and ratios. In most cases, the amount of energy produced peaks around solar noon, having increased steadily from 8:30 a.m. (12:00). At 4 o'clock in the afternoon, consumption of energy drops to its lowest point of the day. The data demonstrate that when the flow rate rises, so does the energy. There is an increase in useable energy when the filling ratio is 50% and a helical spring with a core bar is added.

Tank's temperature

Figures (4 & 5) Show the correlations between solar radiation, storage tank temperature, and ambient temperatures using a 50% filling ratio, both with and without a helical spring placed in the core bar, and varied flow rates. The internal tank temperature increased from 29.5 degrees Celsius to 65.5 degrees Celsius and from 28.8 degrees Celsius to 68.8 degrees Celsius without the use of a helical spring with a core bar at flow rates of 1 l/min and 1.5 l/min, respectively.. Increased usable energy is achieved by increasing the filling ratio to 50% and then inserting a helical spring around a central bar. When the flow rate was 1 L/min, the temperature in the storage tank rose to 73.7 °C; when it was 1.5 L/min, the temperature rose to 76 °C. This effect is caused by the fact that even when solar radiation declines after midday, the temperature in the storage tank remains elevated until 3:30 in the afternoon. The thermosyphon's vapor-working liquid, along with the collector's heat capacity effect, is responsible for this behavior. As predicted, the temperature in the storage tank declines after 3:30 PM, due to the reduction in solar radiation after sunset and the rise in ambient temperature that causes a greater loss of thermal energy from the storage tank. When a helical spring containing a core bar is introduced, the filling ratio increases to 50%, and the temperature rises to 1.5 L/min from 1 L/min.

Temperature distribution

Figures (6 & 7) demonstrate that both the intake and the discharge temperatures are rising considerably before midday. Temperatures continue to rise until around 3:30 p.m., despite the fact that sun exposure decreases during the day. The vapor working liquid inside the thermosyphon causes this behavior because of the heat effect stored in the collector. After 3:30 p.m., the temperature naturally drops as the sun's rays get weaker in preparation for nightfall. The findings show that a boost in flow rate decreased heat loss to the environment. Heat could be transferred from the absorber plate to the fluid at a faster rate if the flow rate were higher, and the system could absorb more energy if the filling ratio was 50% and a helical spring with a core bar had been installed.

Efficiency

Figures (8 & 9)graph efficiency as a function of filling ratio and flow rate on a sunny day. Heat lost to the environment is reduced when flow rate increases. This is because a lower temperature differential between the collector absorber and the ambient environment contributes to higher daily efficiency, and a higher flow rate takes more energy from the absorbing plate. In addition to wind speed, the number of covers, the kind of insulators used, the amount of solar radiation received, and the cleanliness of the weather, a number of other factors affect thermal losses. As can be seen from the data, using a helical spring with a core bar increases efficiency by 50% for a filling ratio of 50%, and by a factor of 0.5 for a flow rate of 1.5 L/min compared to 1 L/min.

ISSN: 2710-2165

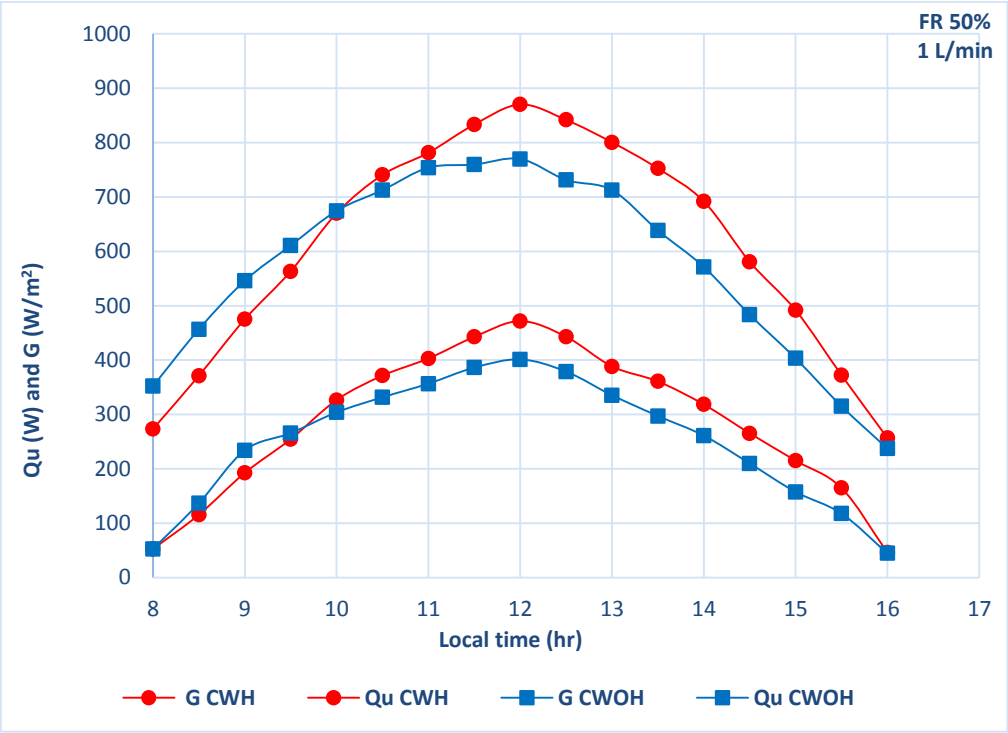

Figure (2) Evaluate the solar radiation and useable energy for a (50%) filling ratio and a (1) L/min flow rate with and without an enhancement device.

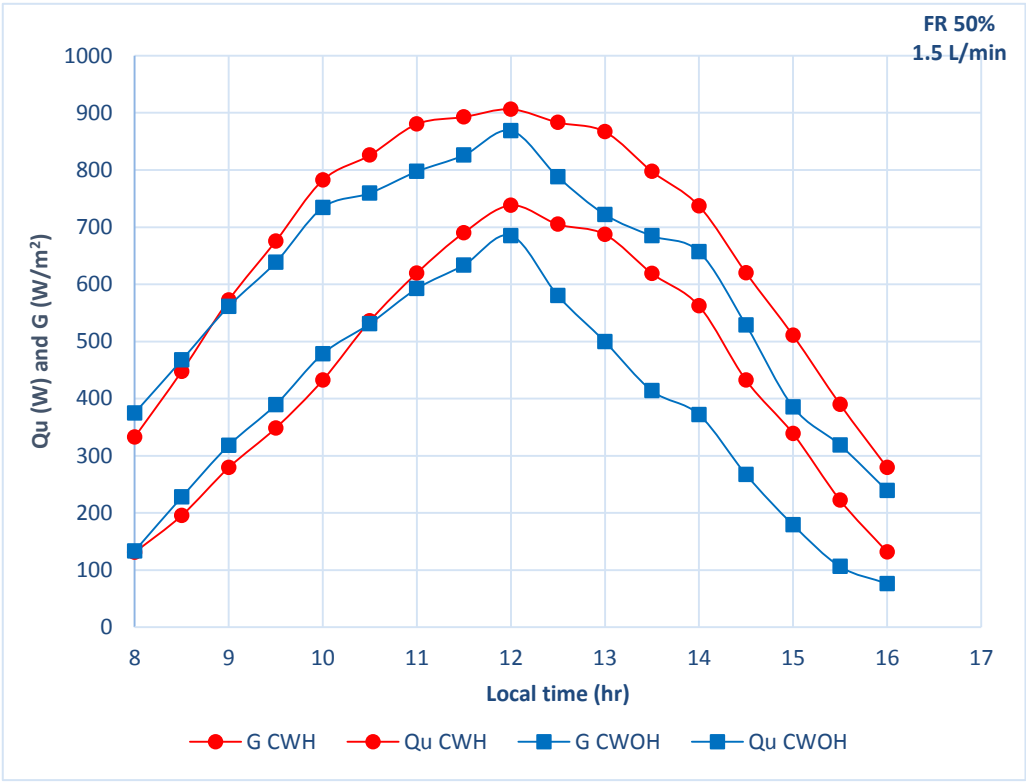

Figure (3) Evaluate the solar radiation and useable energy for a filling ratio of (50%)and a flow rate of (1.5) L/min, both with and without the aid of an enhancement device.

ISSN: 2710-2165

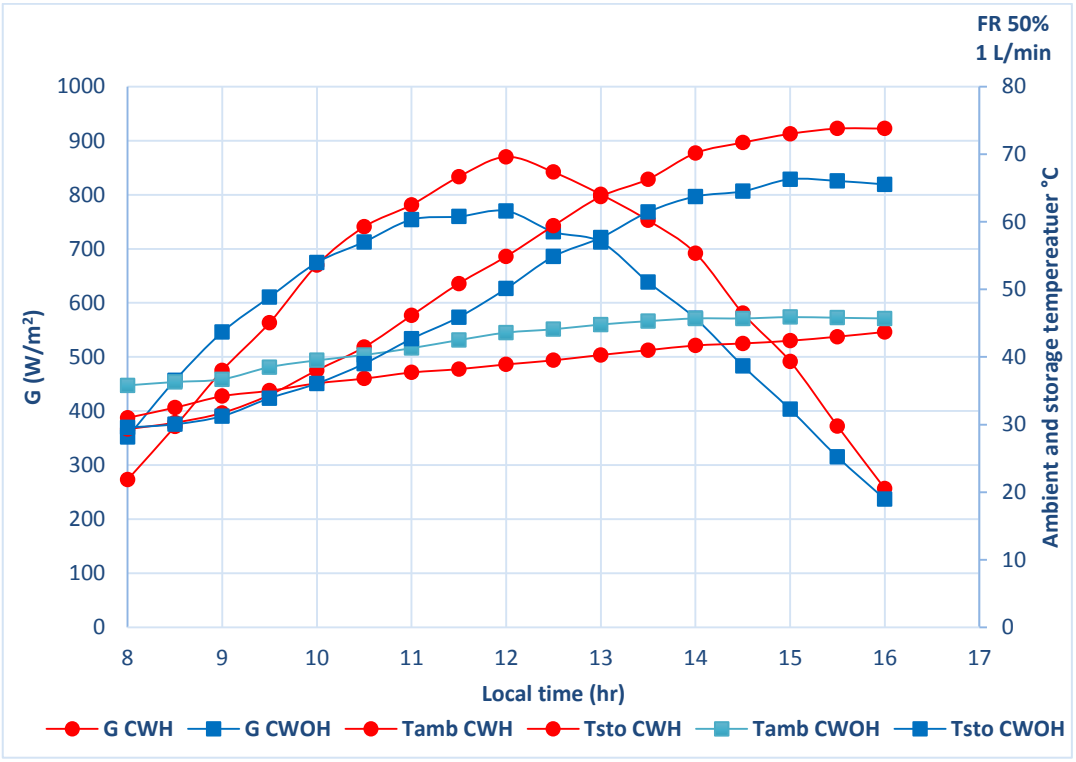

Figure (4) Evaluate the difference between the useable energy and solar radiation for a filling ratio of (50 %) and a flow rate of (1) L/min, with and without an enhancement device.

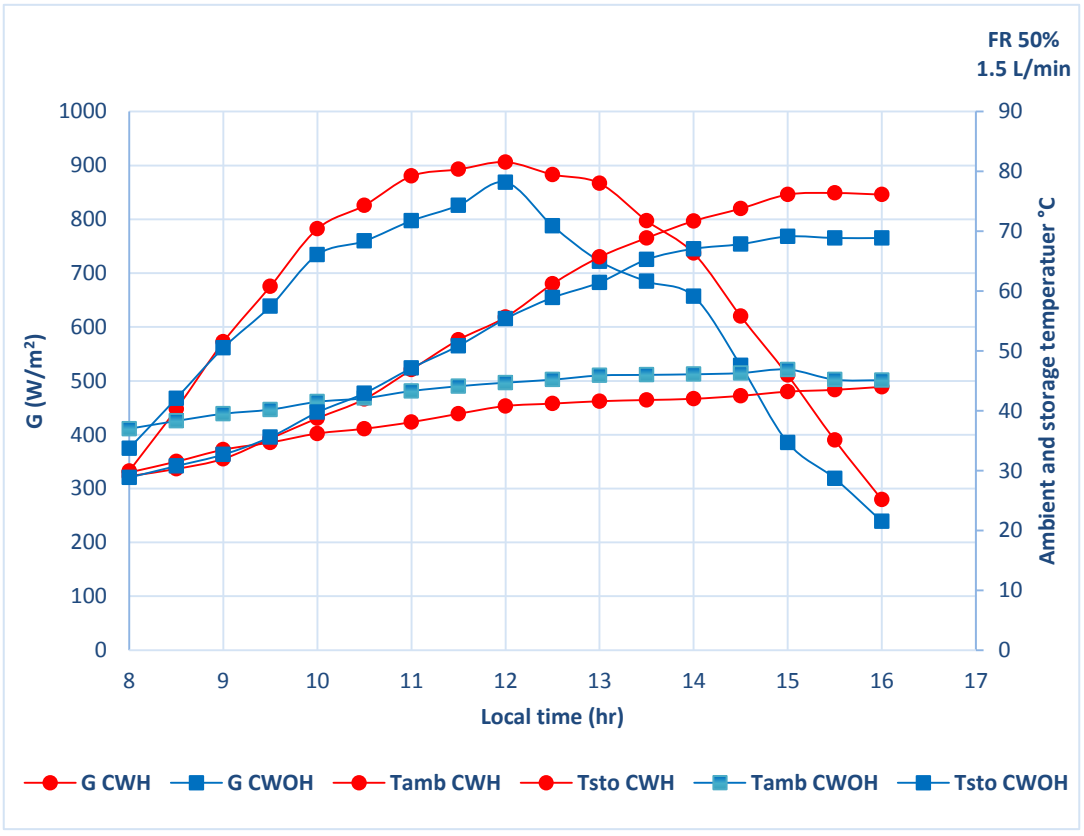

Figure (5) Evaluate the difference between the useable energy and solar radiation for a filling ratio of (50 %) and a flow rate of (1.5) L/min, with and without an enhancement device.

ISSN: 2710-2165

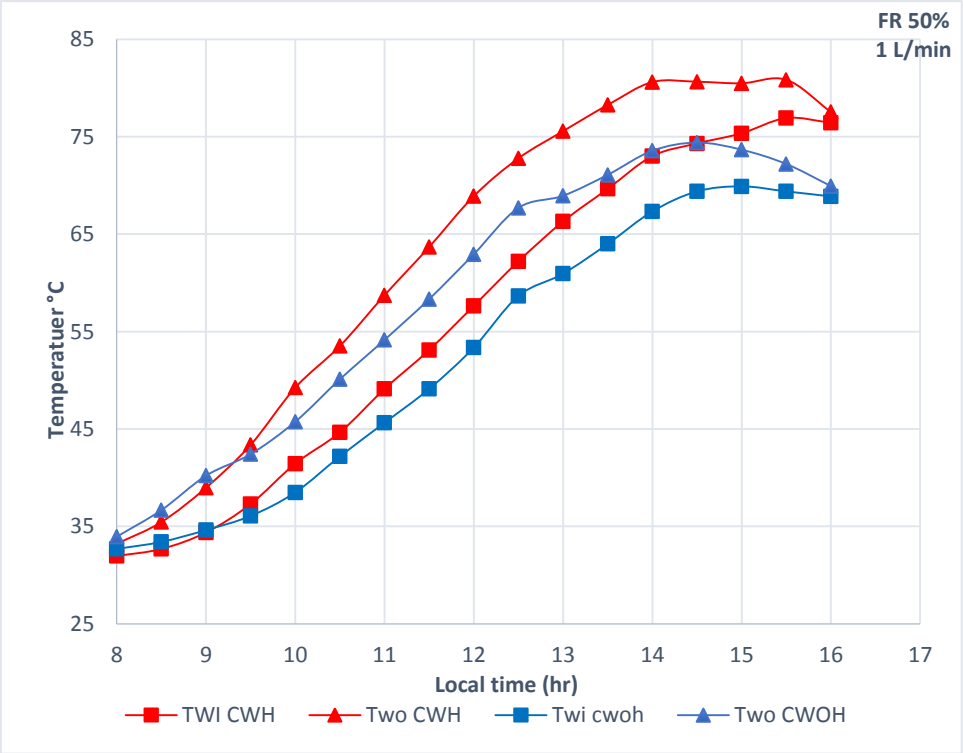

Figure (6) Evaluate the difference between the inlet and exit water temperatures (Twi and Ti) for a filling ratio of (50 %) and a flow rate of (1) L/min, with and without an enhancement device.

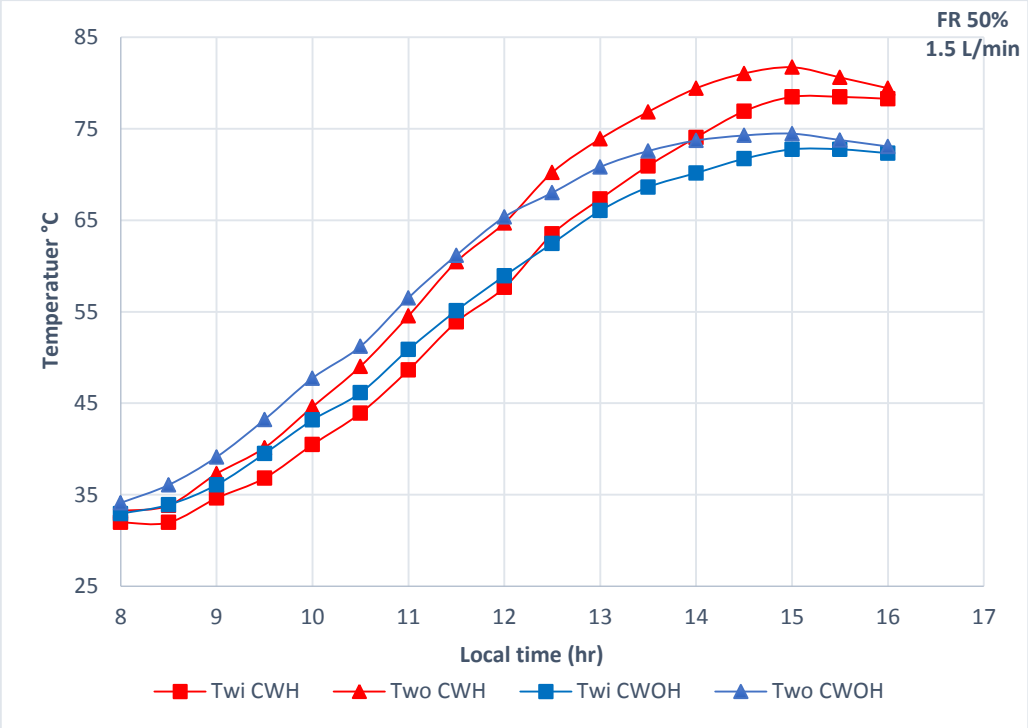

Figure (7) Evaluate the difference between the inlet and exit water temperatures (Twi and Ti) for a filling ratio of (50%) and a flow rate of (1.5) L/min, with and without an enhancement device.

ISSN: 2710-2165

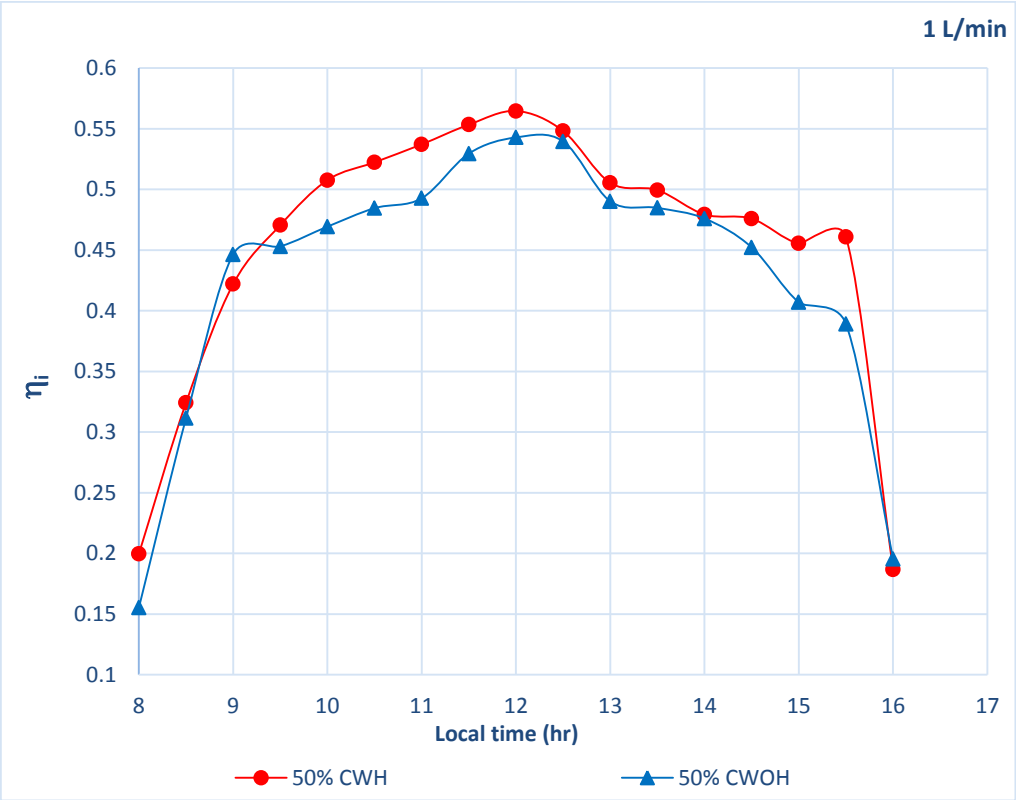

Figure (8) Measure the efficiency for filling ratio of (50%) and a flow rate of (1) L/min with and with enhancement device

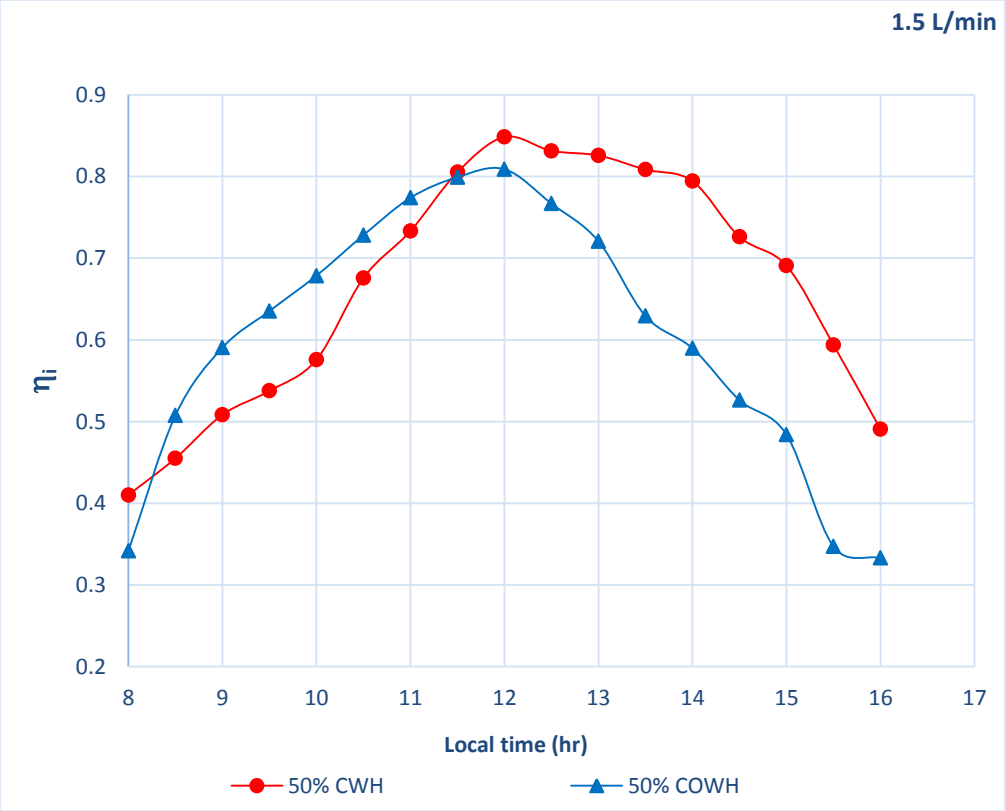

Figure (9) Measure the efficiency for filling ratio of (50%) and a flow rate of (1.5) L/min with and with enhancement device

ISSN: 2710-2165

IV. CONCLUSION

The experimental study of thermosiphon riser solar collector was with different flow rates and filling ratios. The maximum daily efficiency of thermosiphon riser solar collector reached (70%) from falling ratio (50%) at flow rate (1.5 L/min) with enhancement device. The daily efficiency in case of filling ratio (50%) at flow rate (1.5 L/min) with enhancement device increases by (7%) than without the enhancement device . The storage tank temperature increased by (14%)when its work with filling ratio (50%) at flow rate (1.5 L/min) with enhancement device more than without .To sum up,This collector is ideal for use in solar water heating systems since it has the required thermal performance.

REFERENCES

[1] Samanci Ahmet, Berber Adnan. Experimental investigation of single-phase and two-phase closed thermosiphon solar water heater systems. J Acad 2011; 6:688–93.

[2] Ong, K. S., & Tong, W. L. (2011). Inclination and fill ratio effects on water filled two-phase closed thermosiphon. In International Heat Pipe Symposium (Heat) (pp. 167-171). Tamkang University Press.

[3] H. Taherian, A. Rezania, S. Sadeghi, D.D. Ganji, Experimental validation of dynamic simulation of the flat plate collector in a closed thermosyphon solar water heater, Energy Conversion and Management, Volume 52, Issue 1, 2011, Pages 301-307, ISSN 0196-8904, https://doi.org/10.1016/j.enconman.2010.06.063.

[4] Aung, N. Z., & Li, S. (2013). Numerical investigation on effect of riser diameter and inclination on system parameters in a two-phase closed loop thermosiphon solar water heater. Energy conversion and management, 75, 25-35.

[5] Lingjiao Wei, Dazhong Yuan, Dawei Tang, Bangxian Wu, A study on a flat-plate type of solar heat collector with an integrated heat pipe, Solar Energy, Volume 97, 2013, Pages 19-25, ISSN 0038-092X, https://doi.org/10.1016/j.solener.2013.07.025.

[6] Nay Zar Aung, Songjing Li, Numerical investigation on effect of riser diameter and inclination on system parameters in a two-phase closed loop thermosyphon solar water heater, Energy Conversion and Management, Volume 75, 2013, Pages 25-35, ISSN 0196-8904, https://doi.org/10.1016/j.enconman.2013.06.001.

[7] Ji Li, Feng Lin, Gengwen Niu, An insert-type two-phase closed loop thermosyphon for split-type solar water heaters, Applied Thermal Engineering, Volume 70, Issue 1, 2014, Pages 441-450, ISSN 1359-4311, https://doi.org/10.1016/j.applthermaleng.2014.05.019.

[8] Shabgard, H., Xiao, B., Faghri, A., Gupta, R., & Weissman, W. (2014). Thermal characteristics of a closed thermosiphon under various filling conditions. International Journal of Heat and Mass Transfer, 70, 91-102.

[9] Davoud Jafari, Sauro Filippeschi, Alessandro Franco, Paolo Di Marco, Unsteady experimental and numerical analysis of a two-phase closed thermosyphon at different filling ratios, Experimental Thermal and Fluid Science, Volume 81, 2017, Pages 164-174, ISSN 0894-1777, https://doi.org/10.1016/j.expthermflusci.2016.10.022.

[10] Davoud Jafari, Sauro Filippeschi, Alessandro Franco, Paolo Di Marco, Unsteady experimental and numerical analysis of a two-phase closed thermosyphon at different filling ratios, Experimental Thermal and Fluid Science, Volume 81, 2017, Pages 164-174, ISSN 0894-1777, https://doi.org/10.1016/j.expthermflusci.2016.10.022.

[11] Zhi Xu, Yaning Zhang, Bingxi Li, Jingqi Huang, Modeling the phase change process for a two-phase closed thermosyphon by considering transient mass transfer time relaxation parameter, International Journal of Heat and Mass Transfer, Volume 101, 2016, Pages 614-619, ISSN 0017-9310, https://doi.org/10.1016/j.ijheatmasstransfer.2016.05.075.

[12] Hainan Zhang, Zichao Shi, Kaitao Liu, Shuangquan Shao, Tingxiang Jin, Changqing Tian, Experimental and numerical investigation on a CO2 loop thermosyphon for free cooling of data centers, Applied Thermal Engineering, Volume 111, 2017, Pages 1083-1090, ISSN 1359-4311, https://doi.org/10.1016/j.applthermaleng.2016.10.029.

[13] A. Allouhi, M. Benzakour Amine, M.S. Buker, T. Kousksou, A. Jamil, Forced-circulation solar water heating system using heat pipe-flat plate collectors: Energy and exergy analysis, Energy, Volume 180, 2019, Pages 429-443, ISSN 0360-5442, https://doi.org/10.1016/j.energy.2019.05.063.

[14] Shahab Bazri, Irfan Anjum Badruddin, Mohammad Sajad Naghavi, Ong Kok Seng, Somchai Wongwises, An analytical and comparative study of the charging and discharging processes in a latent heat thermal storage tank for solar water heater system, Solar Energy, Volume 185, 2019, Pages 424-438, ISSN 0038-092X, https://doi.org/10.1016/j.solener.2019.04.046.

[15] S.M. Shalaby, A.E. Kabeel, B.M. Moharram, A.H. Fleafl, Experimental study of the solar water heater integrated with shell and finned tube latent heat storage system, Journal of Energy Storage, Volume 31, 2020, 101628, ISSN 2352-152X, https://doi.org/10.1016/j.est.2020.101628.

[16] Anthony J. Robinson, Kate Smith, Turlough Hughes, Sauro Filippeschi, Heat and mass transfer for a small diameter thermosyphon with low fill ratio, International Journal of Thermofluids, Volumes 1–2, 2020, 100010, ISSN 2666-2027, https://doi.org/10.1016/j.ijft.2019.100010.

ISSN: 2710-2165

[17] Behrooz M. Ziapour, Mohsen Bagheri Khalili, PVT type of the two-phase loop mini tube thermosyphon solar water heater, Energy Conversion and Management, Volume 129, 2016, Pages 54-61, ISSN 0196-8904, https://doi.org/10.1016/j.enconman.2016.10.004.

[18] Ahmed A. Alammar, Raya K. Al-Dadah, Saad M. Mahmoud, Effect of inclination angle and fill ratio on geyser boiling phenomena in a two-phase closed thermosiphon – Experimental investigation, Energy Conversion and Management, Volume 156, 2018, Pages 150-166, ISSN 0196-8904, https://doi.org/10.1016/j.enconman.2017.11.003.

[19] Marco Azzolin, Andrea Mariani, Lorenzo Moro, Andrea Tolotto, Paolo Toninelli, Davide Del Col, Mathematical model of a thermosyphon integrated storage solar collector, Renewable Energy, Volume 128, Part A, 2018, Pages 400-415, ISSN 0960-1481, https://doi.org/10.1016/j.renene.2018.05.057.

[20] Eltaweel, Mahmoud; Abdel Rehim, Ahmed A.; Hussien, Hazem (2020). Indirect thermosiphon flat plate solar collector performance based on twisted tube design heat exchanger filled with nanofluid. International Journal of Energy Research, er.5146–. doi:10.1002/er.5146.

[21] Wei-Wei Wang, Yang Cai, Lei Wang, Cheng-Wei Liu, Fu-Yun Zhao, Mikhail A. Sheremet, Di Liu, A two-phase closed thermosyphon operated with nanofluids for solar energy collectors: Thermodynamic modeling and entropy generation analysis, Solar Energy, Volume 211, 2020, Pages 192-209, ISSN 0038-092X, https://doi.org/10.1016/j.solener.2020.09.031.

[22] Jasim, Ayoob Khalid; Freegah, Basim; Alhamdo, Mohammed Hamed (2020). Numerical and experimental study of a thermosyphon closed loop system for domestic applications. Heat Transfer, htj.21877–. doi:10.1002/htj.21877.

[23] Manova, Stephen; Asirvatham, Lazarus Godson; Nimmagadda, Rajesh; Bose, Jefferson Raja; Wongwises, Somchai (2020). Feasibility of using multiport minichannel as thermosyphon for cooling of miniaturized electronic devices. Heat Transfer, htj.21855–. doi:10.1002/htj.21855.

[24] K. Varun;U. C. Arunachala; (2020). Transient parametric pilot study on thermosyphon heat transport device: A computational fluid dynamics hypothesis and experimental exploration. Heat Transfer, doi:10.1002/htj.22035.

[25] Aljuboori, Adeeb A. A.; Ahmed, Saba Y.; Jabbar, Mohammed Y. (2020). Experimental study of closed loop thermosyphon with a different evaporator geometry. Heat Transfer, htj.21887–. doi:10.1002/htj.21887.

[26] Mahasidha R. Birajdar;C. M. Sewatkar; (2021). Experimental investigation of the loop thermosyphon with different adiabatic lengths charged with different working fluids. Heat Transfer. doi:10.1002/htj.22070.

[27] Mousa M. Mohamed, Tarek A. Ghonim, Mostafa A. Abdel-Baky, Karima A. Solima, (2019). Experimental Study of Solar Water Heaters with Heat Pipes. Tenth Conference of Sustainable Environmental Development. 16-20 March 2019. Sharm El Sheikh, Egypt.

[28] Mousa M. Mohamed, Mostafa A. Abdel-Baky, Tarek A. Ghonim, and Karima A. Soliman, (2020). Experimental and Theoretical Study of the Performance of Solar Water Heaters with Gravity-Assisted Heat Pipes. Engineering Research Journal, Vol. 43, No. 1, January 2020, PP: 51-61. Faculty of Engineering, Menoufia University, Egypt.

[29] Duffie, J. A. (2013). WAB (2013). Solar Engineering of Thermal Processes.